

Signal/noise separation in dip space

Richard Ottolini

Seismic signals may be distinguished from noise by examining the dip spectrum at every point. A near-linear seismic event will appear as a peak in the dip spectrum. Noise has a much broader spectrum.

Effective and efficient dip decomposition

The success of this method of signal/noise decomposition is dependent upon effective dip decomposition. An earlier attempt (Claerbout, et. al., 1982) failed because the computation of the dip spectrum by Fourier fan filters could not be sufficiently localized for each data point. Since then two slant stack algorithms have been investigated with better results.

Cross-stacking

Tang et. al. (1983) introduced the method of *cross-stacking* to transform the data into (p, x) space.

$$u(p, x) = \int^t d\tau u(p, \tau)u(x, \tau) \quad (1)$$

where

$$u(p, \tau) = \int dx u(x, \tau = t - px).$$

This equation gives rise to the algorithm illustrated in Figure 1.

The data is first slant stacked to obtain a reference trace $u(p, \tau)$. Then each trace of the linearly moved out (LMO) data is multiplied by the reference trace to give (p, x, τ) space. Finally, these are integrated in time to obtain the desired (p, x) result.

An attraction of this method is its low cost. The cross-stack stage is about the same cost as a slant stack. Instead of slant stacking about every x location, the cost is only that

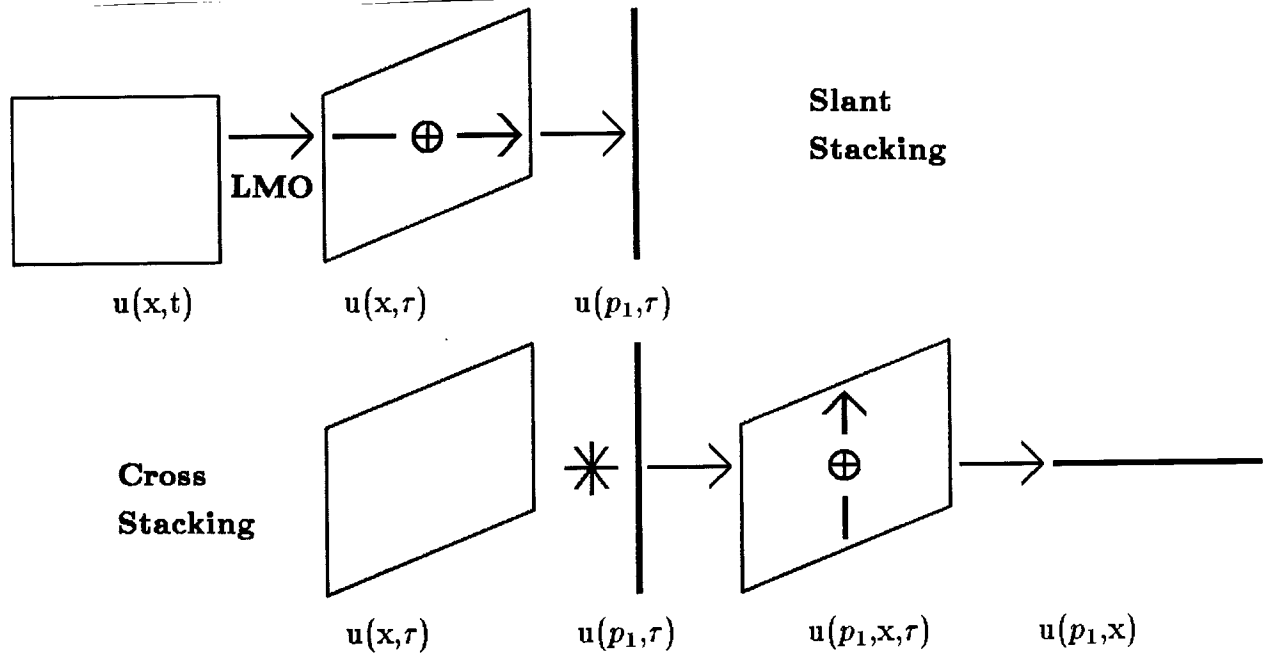


FIG. 1. Tang's method includes a slant stacking step (above) and cross stacking step (below).

of two slant stacks.

This algorithm is modified in a number of ways to obtain the instantaneous dip spectrum. First, the final integration over time is dropped. The (p, x, τ) stage is almost what we want. Inverse LMO is applied to obtain the desired dip spectra (p, x, t) (Figure 2).

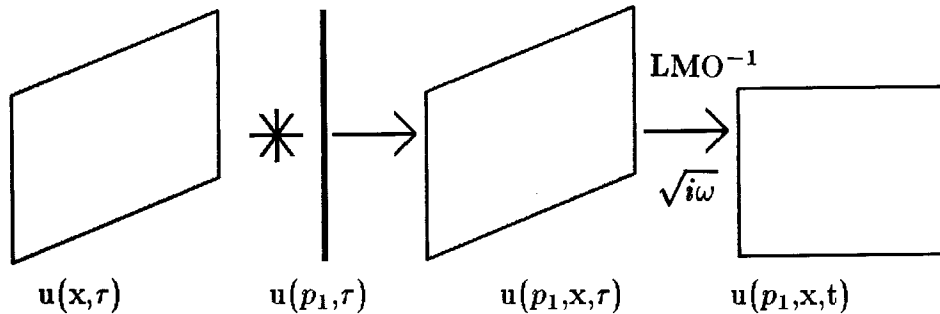


FIG. 2. Modified cross stacking for determining instantaneous dip spectra.

The algorithm of equation 1 contains a couple of amplitude inaccuracies. First, the sign of the data is lost. Second, a sharpening filter must be applied to the reference trace in order to align it with the source data. (A $\pi/4$ point source phase shift correction (Phinney and Frazier, 1981) may be added too.)

Equation (1), modified for dip decomposition is

$$u(p, x, t) = \text{sign} [u(x, t)] \left[\frac{d}{dt} H^+ \right]^{\frac{1}{2}} u(p, \tau + px) u(x, t). \quad (2)$$

The Jacobian notation $\frac{d}{dt}H^+ = \sqrt{i\omega}$ is from Phinney and Frazier.

Equation (2) can be inverted to obtain the original data in the same sense that ordinary slant stacks are invertible. The ordinary inverse involves an inverse LMO, sum across p , and application of the sharpening filter (Figure 3).

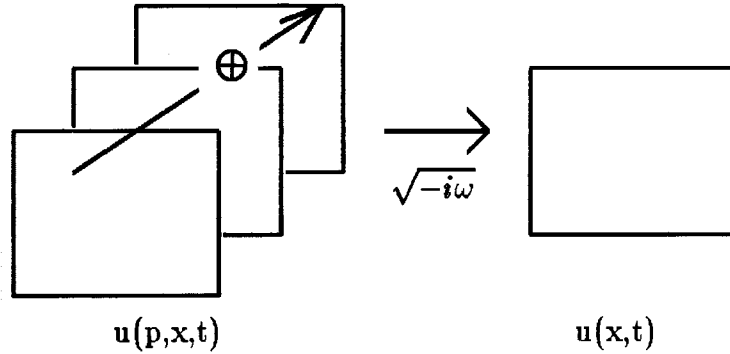


FIG. 3. Inverse slant stacking.

In the case of dip decomposition, inverse LMO has already been applied. So all one need do is to sum over p . Since each slant stack reference trace was multiplied by the original trace, the inverse will be multiplied by the original trace and be the original trace squared. Therefore the inverse of equation (2) is

$$\bar{u}(x, t) = \sum_p u(p, x, t) \tag{3a}$$

$$u(x, t) = \left[\frac{d}{dt}H^+ \right] \text{sign} [\bar{u}(x, t)] \sqrt{|\bar{u}(x, t)|} \tag{3b}$$

In practice, this procedure gives good results on simple synthetics (Figure 4), but limited results on real data. This is due to the global nature of the reference slant stack. Any high amplitude noise spike or seismic event will dominate the slant stack and leave a linear streak on the cross stack.

Local slant stacks

There turns out to be a method of computing local slant stacks for each x location that turns out to be only twice the work of computing the entire slant stack. This method is similar to the dip mix of Robinson and Robbins (1978). The procedure is shown in Figure 5.

The input to the slant stack is a swath of traces centered about the output location x_i . If p is the outer loop in the computation instead of x , then the same input trace can

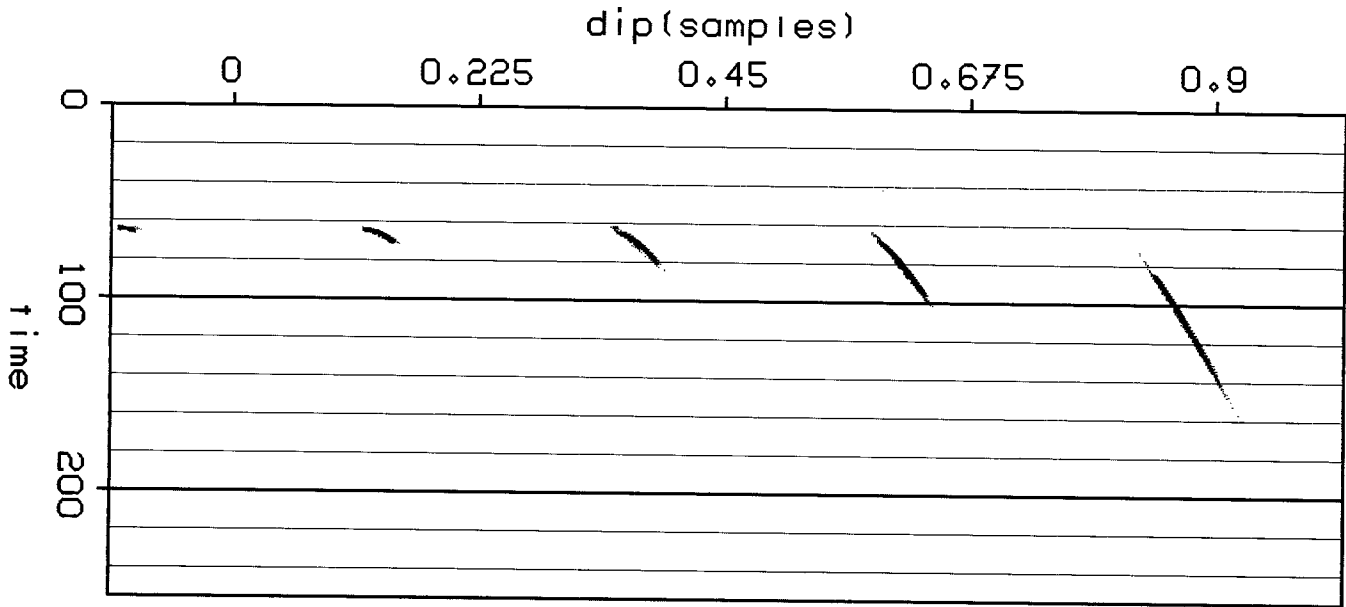


FIG. 4. Dip decomposition of synthetic hyperbola by method of cross-stacking.

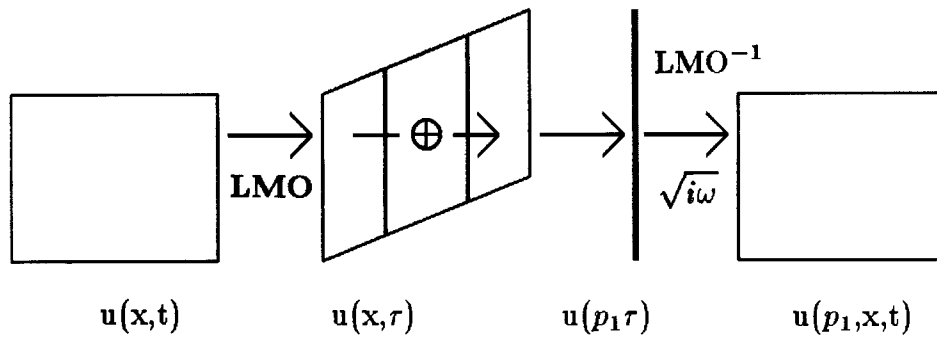


FIG. 5. An efficient local slant stack algorithm.

be used many times with the same LMO adjustment. Also a rolling slant stack is used. As one advances the stacking swath to the next x location then only one trace need be added to the advancing side and one trace subtracted from the other side.

The free parameter in this procedure is the width of the swath. An average Fresnel zone width (which changes with depth) is suggested. This width may be computed analytically or measured experimentally. Beyond some swath width slant stacking stops increasing the power of the slant stack.

Signal/noise decomposition

Figure 6 shows a dip decomposed piece of seismic data. One can see the spikiness of

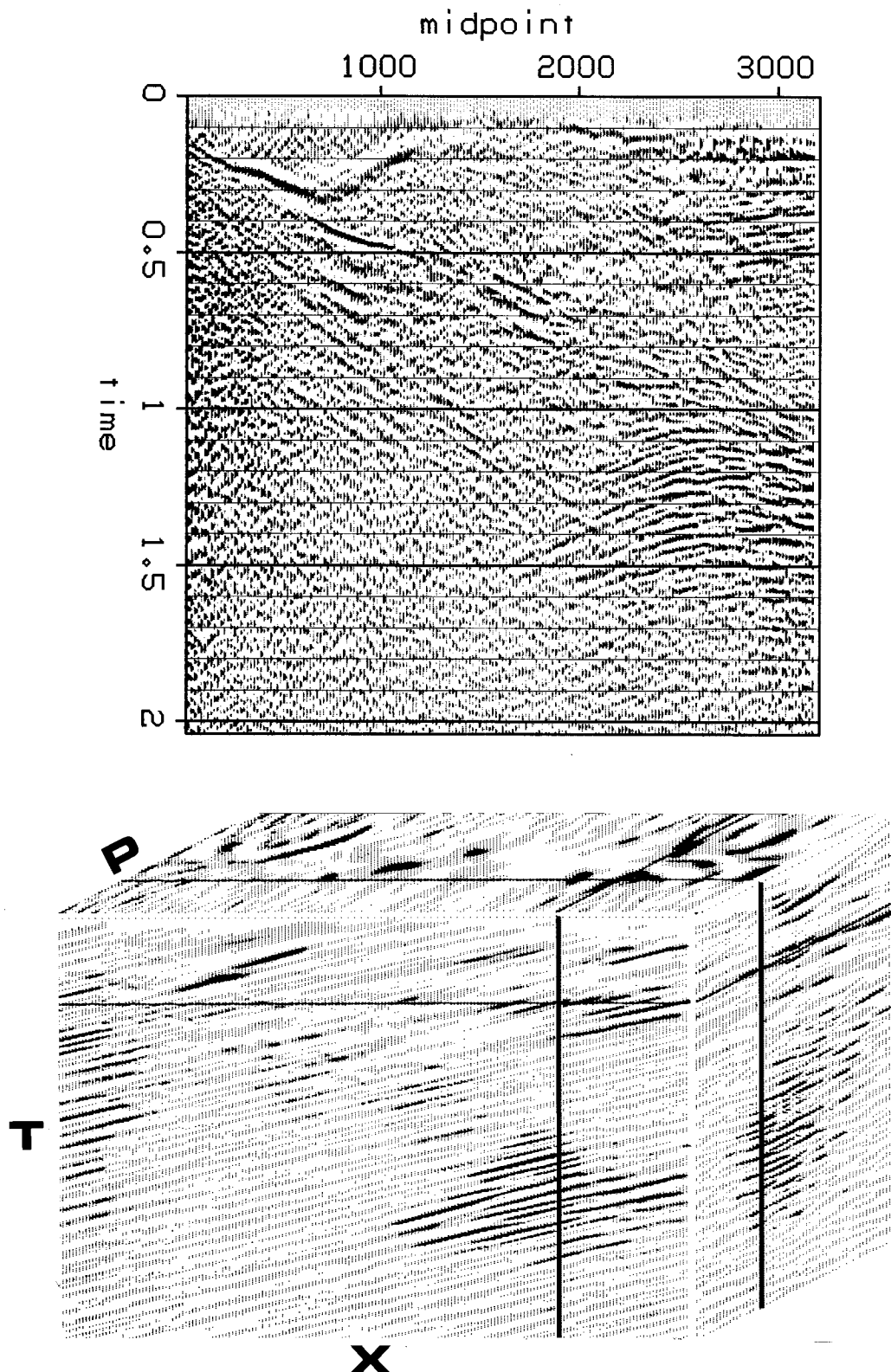


FIG. 6. On top is the source seismic section. Beneath it is a (p, x, t) cube. The front is a dip decomposed section, the side is a localized slant stack, and the top is a (p, x) surface.

the data in the (p, t) plane.

In order to separate signal from noise a spiking statistic was computed for each (x, t) point. The simple generalized norm (Gray, 1979) was used.

$$\frac{\sum_p |u|^\alpha}{\left(\sum_p |u^\alpha|^2\right)^{\frac{\alpha}{2}}} \quad (4)$$

An $\alpha = 3$ value seemed optimal on this dataset. The statistic was smoothed over adjacent points. Then about an arbitrary threshold the spiking statistic selected a signal point. Figure 7 shows a seismic section from which much noise has been removed.

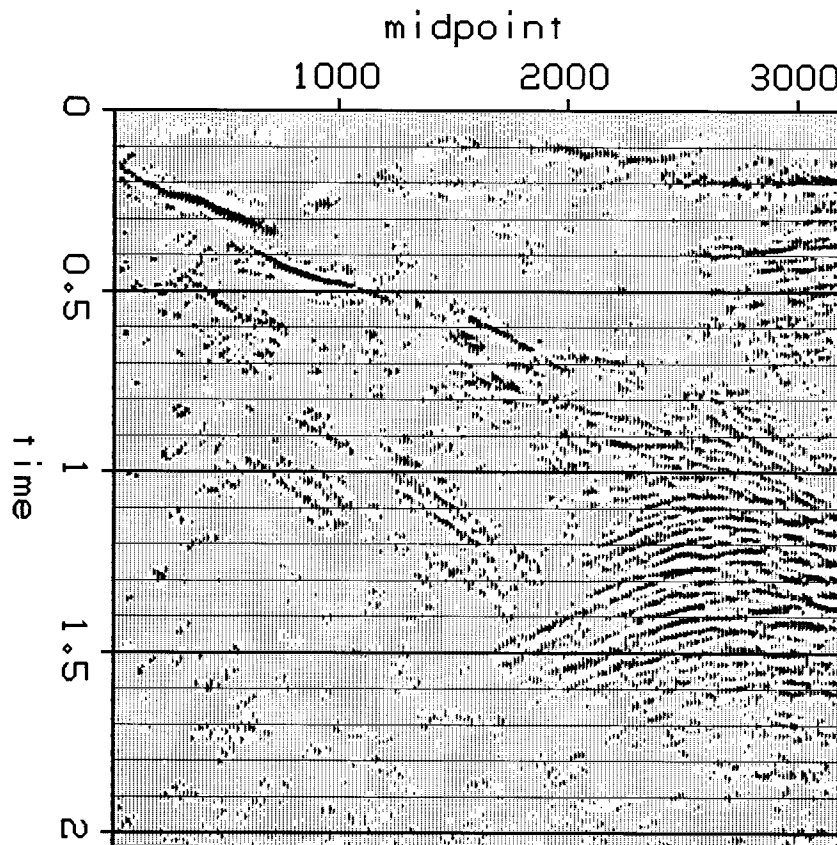


FIG. 7. The same data as Figure 6, except with some noise removed.

Of course, more sophisticated peak detectors can be used in place of the generalized norm. The peak itself may be extracted rather than thresholding the source data. In regards to the threshold method, Harlan's (1983a) method of determining the threshold from artificially whitened data suggests a less arbitrary approach than above.

Other applications of instantaneous dip spectra

The relatively efficient dip spectra decomposition algorithms presented in this paper could be used in other applications. A few are:

- Harlan discusses a (p, x, t) version of his dip decomposition method elsewhere in this SEP report.
- Robinson and Robbins (1978), Levin (1980), Sword (1981), and Harlan (1983c) migrate dip decomposed data.
- Ottolini presents a velocity independent stacking-migration method elsewhere in this SEP report.
- McMechan (1983) and Tang et. al. (1983) estimate velocities from (p, x) curves.
- Paulsen and Merdler (1978) presented a method of automatic reflector picking based upon data dip decomposition.

REFERENCES

- Claerbout, J.F., Harlan, W.S., Ottolini, R., Toldi, J. and Ullmann, R., 1982, Signal/noise decomposition.
- Gray, W.C., 1979, Variable norm deconvolution: SEP-19.
- Harlan, W.S., Claerbout, J.F., and Rocca, F., 1983a, Extracting velocities from diffractions: SEP-32, p. 107-126.
- Harlan, W.S., 1983b, Signal/noise separation and velocity inversion: SEP-37.
- Harlan, W.S. and Burridge, R., 1983c, A tomographic velocity inversion for velocity data: SEP-37.
- Levin, S., 1980, A frequency/dip formulation of wave theoretic migration in stratified media: in Acoustic Imaging, v. 9, p. 681-698, Wang, editor, Plenum Press, N.Y..
- McMechan, G.A., 1983, P-x imaging by localized slant stack of t-x data: Geophysical Journal of the Royal Astronomical Society, v. 72, p. 213-221.
- Ottolini, R., 1983, Velocity independent seismic imaging: SEP-37.
- Paulson, K.V. and Merdler, S.C., 1968, Automatic seismic reflection picking: Geophysics, v. 33, p. 431-440.
- Phinney, R.A., Chowdhury, K.R., and Frazier, L.N., 1981, Transformation and analysis of record sections: Journal of Geophysical Research, v. 86, p. 359-377.
- Robinson, J.C. and Robbins, T.R., 1978, Dip domain migration of two dimensional seismic profiles: Geophysics, v. 43, p. 77-93.
- Sword, C., 1981, Controlled directional receptivity: SEP-26, p. 289-295.
- Tang, R., Carswell, A. and Moon, W., 1983, Velocity analysis in the p-x plane from a slant stacked wavefield: paper presented at the Canadian Society of Exploration Geophysicists in Calgary, 1983.

